ELECTRON BEAM PHYSICAL VAPOUR DEPOSITION THERMAL BARRIER COATINGS: A COMPARATIVE EVALUATION OF COMPETING DEPOSITION TECHNOLOGIES

Y.Jaslier, S.Alpérine
SNECMA - Materials and Processes Department
Site de Villaroche - Bâtiment 41
77550 Moissy-Cramayel
France

ABSTRACT

The need for improving the performance and maintenance costs of gas turbine engines has led to the development of advanced thermal protection systems for critical components such as high pressure turbine (HPT) blades and vanes. This led to the concomitant development of advanced coating deposition techniques. Electron beam physical vapour deposition (EB-PVD) first made possible the application of corrosion resistant overlay coatings on turbine blades. The EB-PVD technology has since been gaining ever more interest world-wide as it stands as the best industrial technique for the deposition of thermal barrier coatings on first stage HPT aerofoils. The strategic nature of the EB-PVD process means that it has been developing somewhat independently on both sides of the *iron curtain* during the cold war years. Today, both American and ex-USSR technologies are open to the market. This is the object of this paper to compare the two state-of-the-arts both from a deposition process standpoint and from a laboratory evaluation on samples. This evaluation covers structural studies as well as thermal cycling testing. The relationship between the deposition process and the coating functional behaviour is discussed.

INTRODUCTION

In the Western countries, the electron beam physical vapour deposition process was originally developed in the late sixties by Airco Temescal jointly with Pratt & Whitney for the application of overlay type oxidation resistant coatings onto high temperature blades and vanes of jet engines[1]. The so-called MCrAlY's, where M is nickel, cobalt, iron or a mixture thereof, offered then superior environmental resistance compared to diffusion aluminides. In parallel with the development of advanced oxidation resistant coatings, emerged a new class of high temperature coatings designated as thermal barrier coatings. A thermal barrier coating (TBC) is a duplex system consisting of a heat insulating ceramic layer deposited on a bond coat underlayer providing adhesion to the ceramic as well as corrosion resistance to the underlying base alloy. The ceramic coating is commonly yttria-stabilised-zirconia for its low thermal conductivity and high thermal expansion coefficient.

The early application of TBC's was the protection of combustor parts. This application involved applying the ceramic coat on top of an MCrAlY coating used as a bond coat, both deposited by air plasma spraying. One advantage of the air plasma spaying technique is to provide the MCrAlY coating with a rough surface onto which the ceramic coating can mechanically bond. Another advantage of air plasma spraying lies in the heavily microcracked ceramic microstructure it produces which is beneficial in terms of strain tolerance and thermal shock resistance.

Since the potential benefits of thermal barrier coatings were additive to the gains in high temperature strength capability of superalloys and in internal and film cooling technologies, there has been a strong drive to extend the application of TBC's to protecting the aerofoil of high pressure turbine blades and vanes. Unfortunately, the plasma spray process proved inadequate for depositing ceramic coatings onto high pressure turbine (HPT) aerofoils due to the poor coating surface finish retention and cooling hole obstruction problems. It has been alleged that ceramic plasma sprayed coatings had 'insufficient' spallation resistance for this application[2].

In the late seventies/early eighties, the EB-PVD technique was found to be a very interesting potential alternative to plasma spraying for depositing TBC's onto aerofoils. Refractory materials deposited by EB-PVD typically exhibit a unique columnar morphology, which has been vehicled as a key feature to accommodate the thermal expansion mismatch strains with the metallic substrate upon thermal cycling and to resist severe thermal shocks. A second advantage of the electron beam physical vapour deposition process is its capability to produce coatings with an acceptable surface finish as-deposited which is retained in service in spite of the erosive environment. A third and not least advantage is that the EB-PVD technique makes controllable and reproducible the obstruction of cooling holes. This is due to the deposition mechanism that takes place through the condensation of coating vapour in the EB-PVD process rather than through the impingement of large semi-molten particles in the plasma spray process.

Although the potential of EB-PVD TBC's was recognised, the know-how to reliably produce TBC's by electron beam physical vapour deposition proved to be arduous to establish because of 'infant mortality' problems as reported by the Western pioneers themselves[3,4]. The strategic nature of the EB-PVD applications means that the difficulties have been tackled and the process technology matured somewhat independently on both sides of the *iron curtain* during the cold war years. Companies such as Airco Temescal, Pratt and Whitney and Chromalloy made essential contributions to make the technology of EB-PVD TBC's industrially viable[4]. Production coatings have been flying in PWA engines since 1989 [2].

In the Eastern countries, the EB-PVD technology was bred in prestigious institutes such as the Paton Welding Institute in Ukraine and the VIAM in Russia, with industrial recipients such as Saturn and Nickolai Kuznetzov (NK). The first Structure Zone Model for physical vapour deposited coatings was first published in 1963 by Movchan and Demchishin[5] and has been universally referred to since. The design approach of Russian jet engine manufacturers was such that it was not felt there was a need for coating HP vane aerofoils with EB-PVD TBC's. As a result Russian experience in production was bound to coating blades, not vanes[6]. This detail bears some implications on the development of tool design and masking technology (or lack of) in the former

USSR. EB-PVD TBC's applied on single crystal blades have been flying on NK engines[7] since 1985.

Today, both the American end ex-USSR technologies are open to the market. This is the object of this paper to shed some light on how the two state-of-the-arts compare from the technology stand-point. Some of the commonalities and differences in the TBC concept and manufacturing technology are first highlighted. Results from a laboratory evaluation of coatings that are representatives of these technologies are then presented and discussed.

COMMONALITIES AND DIFFERENCES

TBCconstituents

Whether they originate from the East or from the West, EB-PVD TBC's have overall much in common if one considers that they all consist of an oxidation resistant bond coat overlaid with a ceramic top coat deposited by electron beam physical vapour deposition. Typical bond coats are from the MCrAlY type. Only in the West, does it appear that diffusion aluminides have been used as bond coats beside MCrAlY's. The range of thicknesses for the MCrAlY and ceramic layers are typically 75-125 and 80-250 microns respectively. Another invariant between the two technologies is the standard ceramic composition which consists of ZrO_2-6to8wt%Y_2O_3 (YSZ). It is interesting to note that this composition range was originally selected from the thermal cyclic life optimisation of TBC's deposited by plasma spraying[8].

The EB-PVD manufacturing process

In generic terms, the EB-PVD process involves evaporating coating material in a vacuum chamber by means of electron beam heating. The coating vapour so generated condenses on the work piece at high temperature. The coating flux being line-of-sight, the parts are manipulated above the evaporation source to maximise coating coverage.

The design of Western EB-PVD coaters is based on the principle that the evaporating conditions must be kept as steady as possible with no interruptions, with a batch of parts being coated in the deposition chamber at any time of the campaign. This approach implies that the parts must be loaded and pre-heated externally to the deposition chamber. The architecture of Western type EB-PVD coaters is thus generally based on a central deposition chamber with separate pre-heating and unloading chambers (see Figure 1). Although the main concern in this approach is to maximise the coater's productivity and reproducibility, the machine design actually has implications on the deposition physics that govern the coating properties and this must be borne in mind when comparing the two technologies. In the deposition chamber, the parts are maintained at temperature mainly thanks to the radiative heating from the molten pool. For metallics however, where the melt pool surface temperature is not as high as for ceramics, supplementary heating of the parts is provided by a resistive radiator [9,10]. Depending on the coater's design, whether it be Temescal or Leybold, the parts are manipulated in the vapour cloud with various complex motion patterns involving rotation and tilting. One of the specificity of the Western technology though is the bleed, inside the coating chamber, of an oxygen containing gas when depositing ceramics[9,10]. The argument put forward to justify for the need of oxygen bleeding is to compensate for the dissociation of zirconia upon heating which would otherwise lead to some oxygen deficiency.

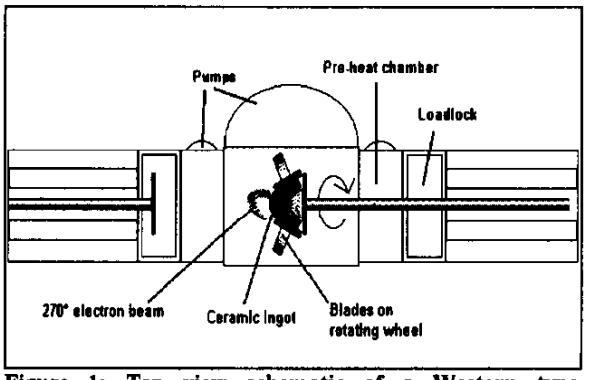

Figure 1: Top view schematic of a Western type (Temescal) production EB-PVD coater[16]

This deficiency is manifested in the black colour of the zirconia coating. The lack of stoichiometry of zirconia deposits is in itself not a problem since it can be restored via a simple heat treatment in air at temperatures as low as 700°C. Some people have claimed that the lack of oxygen during the coating atomic build up actually affected the coating microstructure in a detrimental manner due to the material swelling as a result of restoring its stoichiometry[11]. Another argument for the need of oxygen bleed inside the coating chamber, is the need to establish, prior to depositing the ceramic, a thin film of aluminium oxide at the work piece surface onto which the ceramic condensate can chemically bond[12,13]. The oxygen rich environment surrounding the parts in transit from the pre-heating chamber to the deposition chamber is prone to forming a thin film of alumina acting as the 'glue' of the ceramic coat to be deposited. To the authors, the *in situ* bond coat pre-oxidation prior to ceramic deposition is a stronger argument to justify for the need of oxygen bleed inside the coating chamber rather than stoichiometry or microstructure of the deposit. Yet, the Eastern technology of EB-PVD TBC's matured without identifying oxygen bleed as a key deposition parameter.

Figure 2 is a schematic of a Russian production coater. Its architecture is based on a central deposition chamber with two load locks on each side. There is no separate preheating chambers as in the Western coaters.

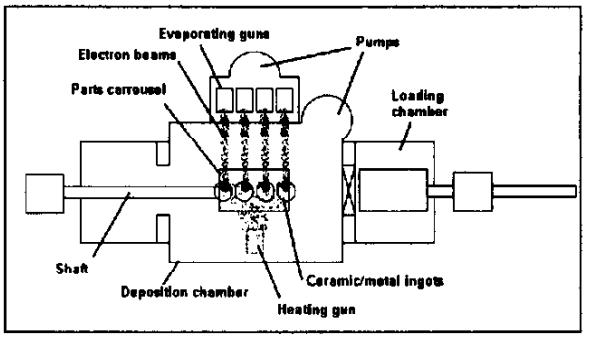

Figure 2: Top view schematic of an Eastern type production EB-PVD coater

Pre-heating of the parts is accomplished inside the deposition chamber by the means of an electron beam gun located in a separate chamber above the deposition chamber. This gun is also used as auxiliary heating of the parts during the coating process. Four stacks of ceramic or metal ingots are positioned in a row and are evaporated by four individual linear electron beam guns. The deposition process is carried out at a vacuum

level of a few 10^{-4} Torr. There is no intentional bleed of a reactive gas into the chamber. A typical coating cycle consists first in mounting the carrousel holding the parts on the driving shaft inside the loading chamber. After the loading chamber has been evacuated, the locking vane is opened and the carrousel with the cold parts is introduced into the deposition chamber by translation of the shaft. The parts are pre-heated inside the deposition chamber by the heating electron beam gun while the evaporating guns are kept shut down. Evaporation is started after the work pieces have reached the right temperature regime. Once the deposition is completed the carrousel is driven back into the loadlock where it is left to cool down before it is unloaded.

It should be noted at this point that Western coaters are generally designed to be dedicated to one type of coatings i.e. metallics or ceramics whereas, in the Eastern art, the coaters are designed and used to deposit both types of coatings. Whether the latter approach is better or worse from the production standpoint than the dedicated type coater approach is not the debate of the present discussion. The point is that the flexibility of the Eastern type coaters permits to evaporate metallics concurrently with ceramics or to deposit both in sequence in the same coating cycle and this is essential to their art[14].

SCOPE OF LABORATORY EVALUATION

Coating systems

Two thermal barrier coating systems were evaluated in this study. The Russian coating was manufactured at the Samara plant of NK Engines under the technical supervision of the VIAM Institute in Moscow. The American thermal barrier coating is the well known RT31/RT33 system manufactured by Chromalloy in the USA. The nominal designation of these systems is given in the table below:

Bond coat/ Top coat Designation	*Bond coat composition*	*Ceramic top coat composition*
RT31/RT33	Co34Ni20Cr8Al0.5Y	ZrO_2-7 wt%Y_2O_3
SDP2/KDP1	Ni20Cr12Al0.5Y	ZrO_2-7wt%Y_2O_3

For each system, both bond coat and ceramic coat were applied by electron beam physical vapour deposition on disk and cylinder shaped test pieces made out of Hastelloy X. The composition of Hastelloy X is given in the table below in wt%:

Ni	Cr	Fe	Mo	Co	W
bal	22	18	9	1	0.2

Characterization

The morphology of the ceramic layers was evaluated using a field emission gun scanning electron microscope (FEG-SEM). Energy Dispersive X-Ray analysis coupled with SEM was used to perform chemical analysis in both the as-deposited and as-tested state. Ceramic phase composition was determined using CuKα X-Ray diffraction.

TBC performance was evaluated using a thermal cycling test. Thermal cycling was conducted on 6 and 10mm diameter bars in a furnace with a cycle consisting of 55 minutes at 1100°C with a 5 minute heat up and 15 minute cool down to room temperature using forced air convection cooling. The probability for the ceramic to spall off after many cycles increases with dwell time at room temperature. This effect, although poorly understood, is known to be moisture related. Other investigators have reported the effect of moisture on the spallation resistance of thermally grown oxides on bare superalloys[15]. In these tests, thermal cycling was interrupted every 20 cycles with the test pieces left at room temperature for a time up to 4 hours, after what the specimens were inspected and the cycling resumed. A dwell time of 4 hours at room temperature was chosen so as to let enough chance for the moisture to have an effect, if any. The failure criterion was a ceramic spalled area of at least 20% of the specimen coated surface.

RESULTS

Characterization of as-deposited TBC's

The overall TBC systems are presented in Figure 3. It may be seen that each ceramic coating system exhibits a specific ceramic morphology. For a same nominal YSZ composition, the RT33 process produces a coarser, more columnar shape morphology compared to the finer, feather-like, KDP1 ceramic morphology. Moreover, the KDP1 feathered columns coarsen towards the outer surface. This effect is not as dramatic in the RT33 morphology.

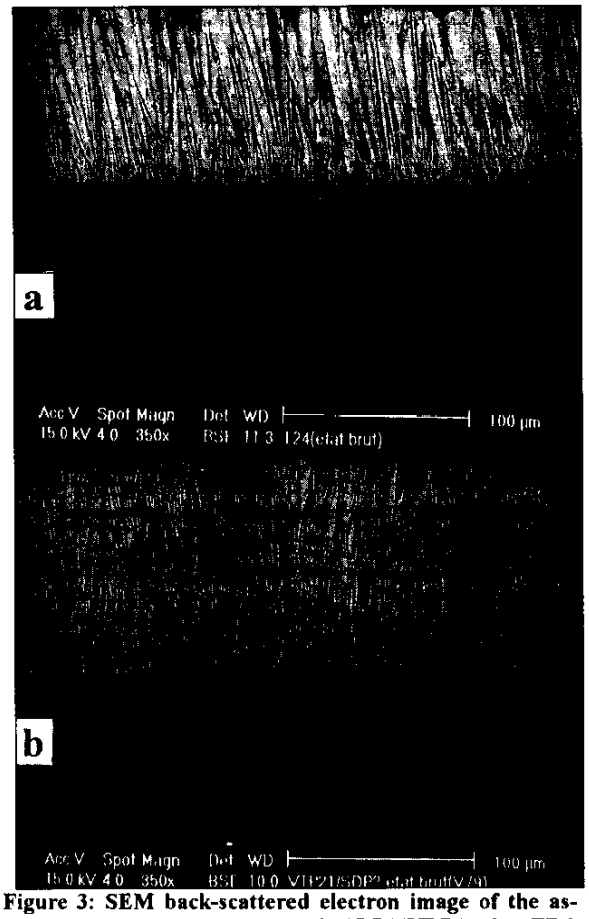

Figure 3: SEM back-scattered electron image of the as-deposited RT31/RT33 (a) and SDP2/KDP1 (b) TBC systems

High magnification examination of the ceramic layers at 50 micron height from the bond coat gives some insight into the column sub-structure (Figure 4). Back-scattered electron imaging reveals internal striation consisting of alternate dark and white layers. This effect is a lot less pronounced in the

case of the KDP1 ceramic where only minor striation may be distinguished in the core centre line of the feathered columns.

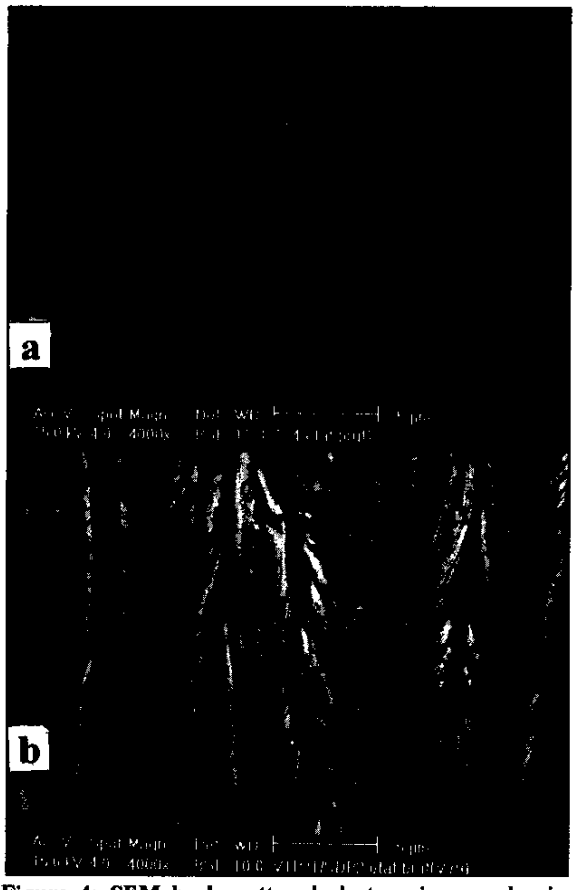

Figure 4: SEM back-scattered electron images showing details of as-deposited RT33 (a) and KDP1 (b) ceramic morphologies.

X-Ray diffraction patterns of each ceramic layer are presented in Figure 5. It was found that each ceramic system was single phased and consisted of the non-transformable tetragonal phase (t').

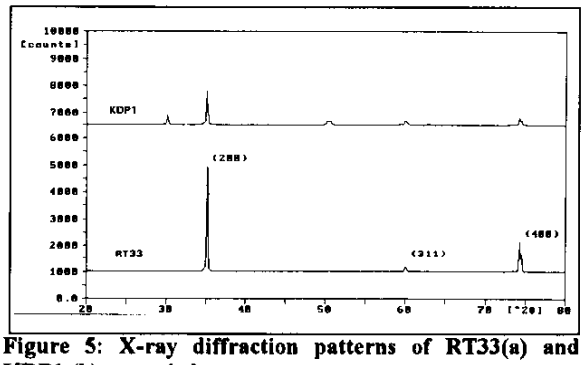

Figure 5: X-ray diffraction patterns of RT33(a) and KDP1 (b) ceramic layers.

All coatings exhibited the (200) preferential growth orientation. This texture is however less pronounced in the Russian ceramic. No peak broadening was observed indicating that the diffracting domains were larger than 0,1 micron in size.

Overall bond coat composition was determined using semi-quantitative EDS analysis over an 80x80microns window centred within the bond coat depth. The analysis results are shown in the table below:

	Co	Ni	Cr	Al	Y	Fe
RT31 wt%	bal	38	18	8.9	<1	<1
at%		34	18	17		
SDP2 wt%	-	bal	14	12	<1	<1
at%			14	22		

A band of white dots identified as yttrium rich precipitates was found at mid-height in the RT31 CoNiCrAlY (see Figure 3). It was observed at higher magnification that this yttrium rich phase was nucleated at the γ/β phase boundary. No such yttrium rich precipitates were observed in the SDP2 NiCrAlY layer. A feature peculiar to the SDP2 MCrAlY layer was the presence of a population of chromium rich nodules of 1 micron in average diameter (see Figure 6). These constituents appeared black in back-scattered electron imaging. Examination in the secondary electron emission mode revealed a surface relief suggesting that these nodules were harder than the matrix. These observations point to the presence of chromium carbides (Cr_7C_3?,$Cr_{23}C_6$?), indication that would need to be confirmed using X-Ray diffraction.

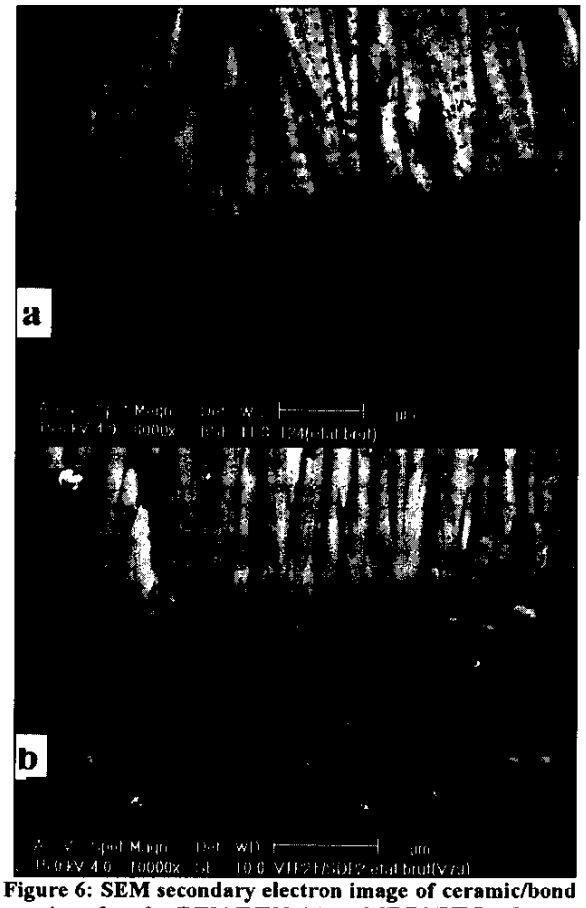

Figure 6: SEM secondary electron image of ceramic/bond coat interface for RT31/RT33 (a) and SDP2/KDP1 (b)

A close examination of the ceramic/bond coat interface reveals that the alumina film developed on the SDP2 bond coat is continuous and thinner than that developed on RT31 (see Figure 6). For the latter, alumina seems to only have formed at the interface with the γ phase i.e. no alumina could

be identified at the YSZ/β-(Ni,Co)Al phase interface using SEM.

Right underneath the alumina film formed on SDP2, there exists a thin (1.5 to 2μm) and very fine grained MCrAlY sub-layer separated from the bulk of the bond coat by a line of alumina inclusions (see Figure 7).

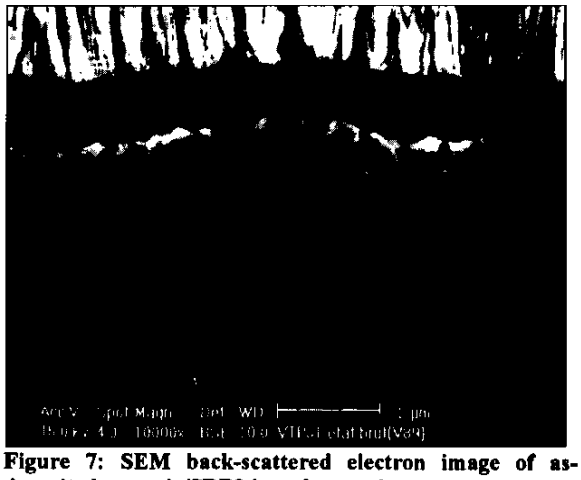

Figure 7: SEM back-scattered electron image of as-deposited ceramic/SDP2 interface region

Thermal cycling performance

Figure 8 is a bar chart showing thermal cycles-to-failure for the SDP2/KDP1 and RT31/RT33 coatings on 10mm diameter bars (unless otherwise stated).

Coating spallation life is found to be very scattered for both systems. There appears however that, under the specific testing conditions used in this study, the SDP2/KDP1 coating overall exhibits a superior spallation resistance compared to that of the RT31/RT33 coating. Mean, low and high thermal cyclic lives are shown in the table below for comparison.

	RT31/RT33	SDP2/KDP1
Low	19	96
Mean	260	460
High	710	1081

Ceramic spallation occurred at room temperature. In most cases, the spallation event was not progressive but abrupt, with typically 80% of the ceramic loss occurring at once from a no spall situation. One exception was the SDP2/KDP1 specimen that was stopped after 1080 cycles. This specimen failed via the occurrence of discrete spalls that were dispersed and small in size (no bigger than 2mm) but the number of which increased with test cycles.

The short life specimens typically exhibited a shiny metallic surface on the substrate surface where the ceramic had spalled. The longer the lifetime of the test pieces and the more grey and mat this surface looked. For the high life specimens, this surface appeared covered with a grey film of dust. This film could be rubbed off with the finger tip. This pattern was generally followed by both the RT31/RT33 and SDP2/KDP1 systems. In two instances with the SDP2/KDP1 coating (96 and 114 cycles), the ceramic free substrate surface and the inner side of the ceramic spalls were blue/green in colour, indicating the presence of nickel and chromium rich oxides. These visual observations were followed with SEM evaluation.

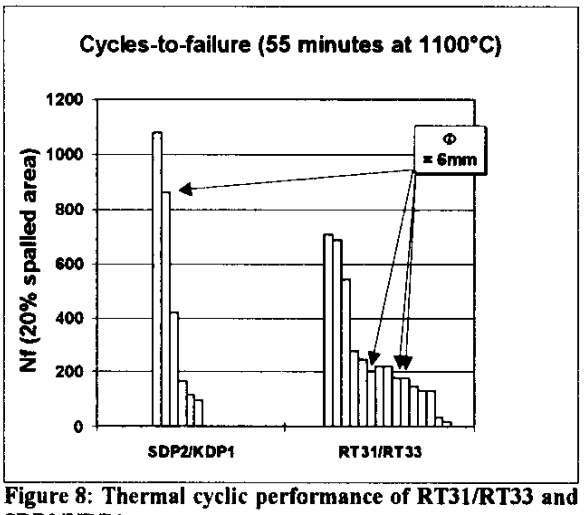

Figure 8: Thermal cyclic performance of RT31/RT33 and SDP2/KDP1 systems

Characterization of as-tested TBC systems

Micrographs of a typical low life (106 cycles) RT31/RT33 system are shown in Figure 9. The substrate surface was analysed and consisted of MCrAlY with small isolated alumina patches. The remnant alumina most often contained yttrium rich oxides that show up as white constituents using atomic contrast imaging. The inner side of the ceramic spall was analysed by EDS and consisted of alumina with isolated yttrium rich oxide phases. The alumina grains imprints can be recognised on the bond coat surface. These observations demonstrate that ceramic spallation occurred through the propagation of a crack running at the MCrAlY/alumina interface breaking off the yttrium rich alumina protrusions.

The failure morphology of low life SDP2/KDP1 coatings was similar to that described above, with the exception that no yttrium rich oxide phases seemed to have formed. In Figure10 are shown micrographs of a SDP2/KDP1 coating failed after 96 cycles. This specimen was peculiar in that a continuous layer of (Ni,Cr,Al) bearing oxides, presumably spinels, had formed between the alumina scale and the ceramic. This mixed oxide layer that appears voided in cross section (Figure 10b) behaved as another site for crack propagation in addition to the MCrAlY/alumina interface.

In Figure 11 are presented micrographs of the RT31/RT33 specimen that failed after 710 cycles. EDS analysis of the inner side of the ceramic spall indicated that it consisted predominantly of YSZ ceramic. Inversely, the substrate surface side consisted mainly of aluminium oxide, implying that cracking had occurred at the ceramic/alumina interface. The respective fractured surfaces reveal a comparable topography consisting of equiaxed spherical grains less than 1 micron in size. Some isolated (Ni,Co,Cr,Al) mixed oxides were also observed at the interface between the ceramic and alumina scale although this feature remained marginal.

The most durable SDP2/KDP1 specimen (1080 cycles) was assessed on a polished cross-section. The progressive failure of this specimen into discrete ceramic spalls did not make possible to look at freshly spalled surfaces. It can be seen in Figure 12a that a crack is running predominantly within the outer region of the alumina scale with some excursions into the ceramic. It cannot be determined whether this crack is the result of metallographic preparation or whether it is a genuine defect generated from the cycling.

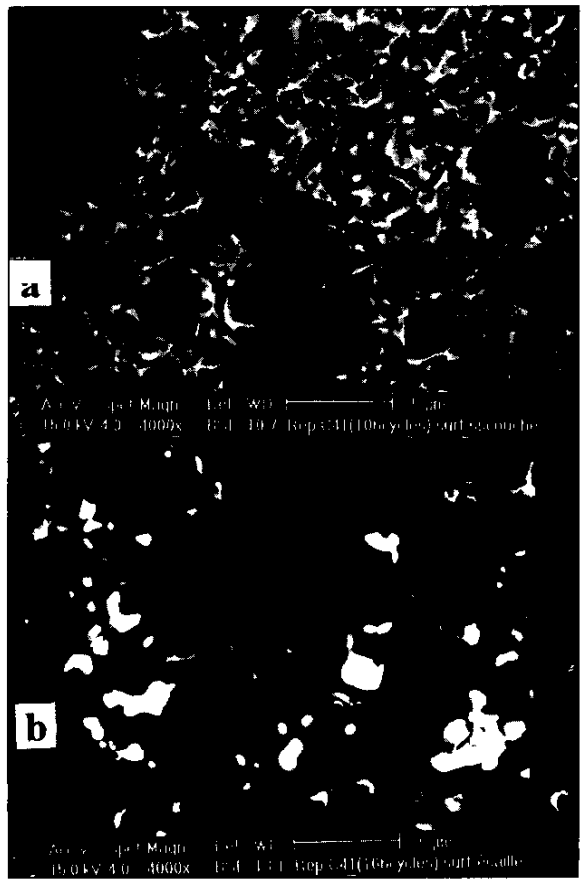

Figure 9: SEM back-scattered electron images of bond coat surface (a) and inner side of ceramic spalls obtained from a low life RT31/RT33 system (b)

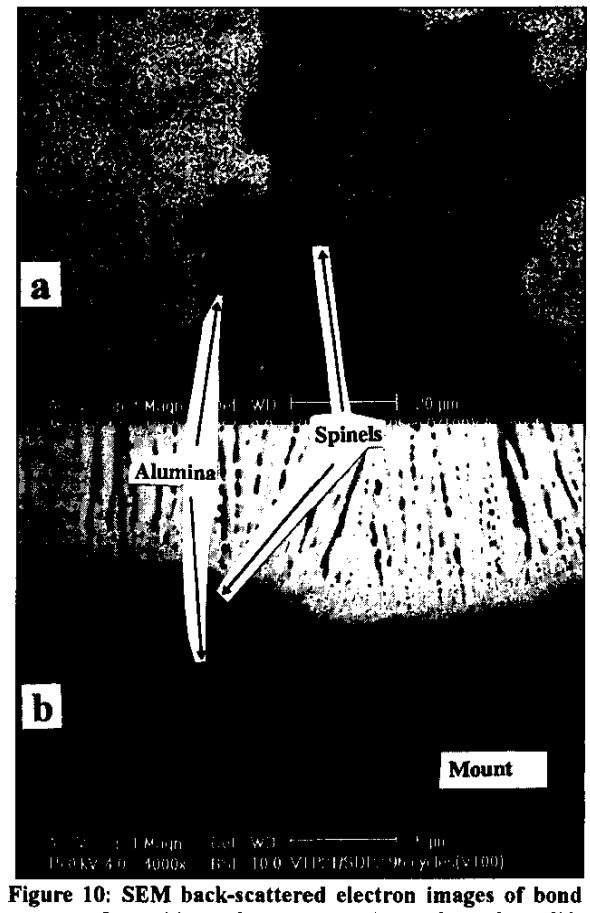

Figure 10: SEM back-scattered electron images of bond coat surface (a) and cross section of a low life SDP2/KDP1 system (b)

Its location however indicates that the ceramic/alumina interface region is the weakest link. Some isolated nodules of (Ni,Cr,Al) mixed oxides were also found to have formed between the alumina scale and the zirconia, locally lifting off the ceramic coat (see Figure 12b). The formation and growth of these mixed oxide nodules may be responsible for the discrete ceramic spalls that were observed on this specimen. The alumina scale thickness on this coating after 1080 cycles was measured at 5.5 microns which is to be compared to the 7.5 microns alumina scale developed on RT31/RT33 after 710 cycles (see Figure 13).

DISCUSSION

As-deposited thermal barrier coating systems

Ceramic considerations

The difference in ceramic morphologies obtained from the RT33 and the KDP1 process clearly demonstrates how sensitive the morphology of EB-PVD deposits can be to specific deposition conditions. Morphology is classically affected by the substrate surface roughness [16,17], substrate temperature [5,17], deposition rate and part motion pattern in the vapour cloud such as rotation speed[18]. No major differences exist in either the deposition temperature range or the bond coat surface finish between the two processes that could account for this effect. The part motion pattern and the vapour cloud distribution inside the coating chamber, both very dependent on the coater design, are however very different. These parameters are therefore potential contributors to the difference in ceramic morphology that is observed. This argument must be put in perspective with the fact that Western EB-PVD TBC's deposited either from a Leybold or a Temescal machine are very similar in morphology[19] with yet massive differences in the coating chamber configuration. The role of chamber pressure and deposition rate (higher in the Western process) on morphology should not be ignored.

Another difference in ceramic structure was found in the column striation which is significant in RT33 but only marginal in KDP1. This well-known feature is usually related to rotation of the work piece during deposition[20]. As the parts are rotated in the vapour cloud, the surface to be coated sees alternate regimes of high deposition rate at high temperature when facing the source (brighter lines) to low deposition rate at lower temperature when facing away from it (darker lines). Lelait et al[21] have identified using transmission electron microscopy that the darker lines corresponded to aligned porosity in the ceramic columns. Later, a 'dynamic sintering' coating growth model has been proposed to account for the presence of intra-columnar porosity in EB-PVD deposits[17]. This model was developed on the consideration that a PVD deposit builds up as a porous atomic network and that this spontaneous defectiveness is overcome at high temperature by diffusion processes resulting in an array of micropores (coalesced vacancies). It was proposed that not only the ceramic surface temperature played a role in the rotation induced striation of the ceramic columns but also the kinetic

energies of the condensing species which were in turn affected by gas scattering effects.

It may be understood that the ceramic striation is less pronounced in the case of Russian ceramics if one considers that:

- the ceramic surface temperature does not fluctuate with rotation as much in amplitude as in the Western process since the part temperature relies to some extent on auxiliary electron beam heating.
- when the surface to be coated faces away from the source, only the thermalised fraction and back scattered molecules of the vapour cloud can possibly deposit. In the KDP1 process, where the evaporation takes place in a vacuum of a few 10^{-4} Torr, the surface to be coated hardly receive any coating flux when facing away from the source.

Unlike morphology, the phase composition was found to be an invariant between the two kinds of ceramic. The finding of the (t') phase in 7YSZ EB-PVD deposits was first established by Lelait et al[21] after previous authors had concluded to the presence of the cubic phase. This phase is typically obtained from quenching the cubic phase of bulk ZrO_2-7wt%Y_2O_3 ceramic[22]. It is also found in plasma sprayed ZrO_2-7wt%Y_2O_3 deposits due to the rapid solidification nature of this process. The formation of the (t') phase in EB-PVD deposits can be explained from the fact that the yttrium and zirconium oxide molecules condense randomly at a relative temperature T/Tm of 0.4 approximately (where T and T_m are the absolute surface temperature and melting point of zirconia respectively). In this temperature regime, cation diffusion is too sluggish to allow for the yttrium to redistribute into the yttrium rich cubic phase and the low yttrium content transformable tetragonal phase. Given that the RT33 and KDP1 processes involve a same ceramic composition (zirconia alloyed with 7wt%yttria) and a low deposition temperature relatively to the melting point of zirconia, one could expect the formation of (t') phase in both ceramic deposits.

The RT33 ceramic deposits exhibited a preferred (200) orientation that was much more pronounced than in the case of KDP1. A zirconia condensate with a (200) texture builds up with atomic layers in the coating plane that consist exclusively of oxygen atoms. It may therefore be argued that the richer oxygen environment characteristic of the RT33 process will favour the (200) growth orientation compared to a deposition process carried out in vacuum.

Bond coat considerations

MCrAlY bond coats are classically described as consisting of β-(Ni,Co)Al precipitates in a solid solution of γ-(Ni,Co)CrAl. Both RT31 and SDP2 bond coats fit this pattern. Some differences were found relative to the presence of a third population of constituents identified as yttrium rich precipitates in the former and presumed chromium carbides in the latter. These differences most probably reflect different bond coat processing histories involving work hardening and heat treatment steps. Some deviation from the nominal composition was noticed in the chromium content of the SDP2 bond coat. This deficiency of a bond coat applied on an otherwise chromium rich substrate, may be partly attributed to chromium evaporation during the vacuum heat treatments at 1050°C that preceded ceramic deposition.

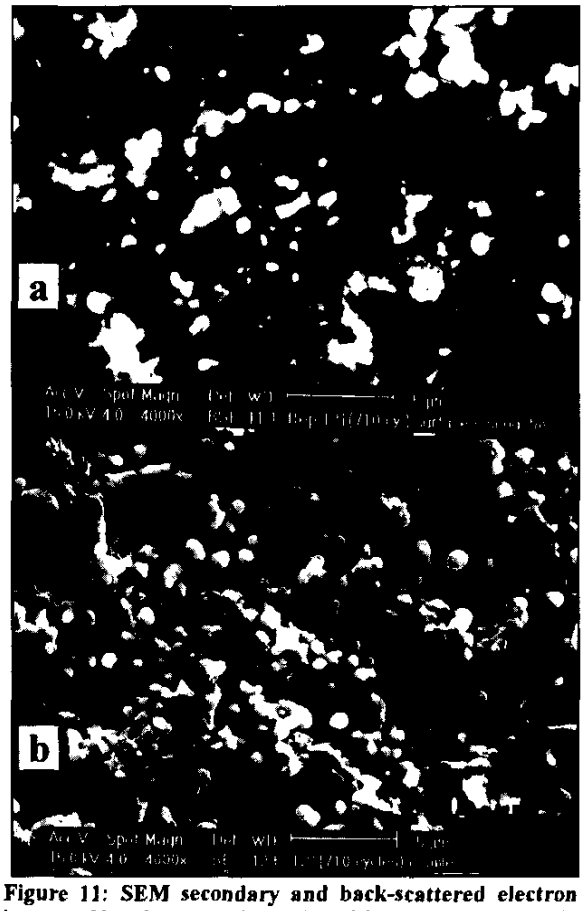

Figure 11: SEM secondary and back-scattered electron images of bond coat surface (a) and inner side of ceramic spalls (b) obtained from a high life RT31/RT33 system

The most peculiar feature that distinguishes the SDP2 bond coat from RT31 is the presence of a fine grained MCrAlY sublayer adjacent to the ceramic coat. This thin layer originates from the evaporation of a flash of MCrAlY on top of the already mechanically prepared and heat treated bond coat surface. The Russian art is such that, for each ceramic deposition run, the evaporation of MCrAlY for tens of seconds precedes the onset of ceramic evaporation. This philosophy probably is meant to deposit the ceramic layer on a fresh, reactive and contaminant free surface.

The nature of the bond coat metal surface is of prime importance as it controls the nucleation and growth of the oxide film that acts as the glue of the ceramic layer. Evidence was shown that this native oxide was different (in thickness and continuity at least) whether it was formed at the RT31/RT33 or SDP2/KDP1 interface.

The interfacial oxide film may form as a result of one or a combination of mechanisms such as:

1. *ex-situ* bond coat oxidation prior to the ceramic deposition step. In both the Western and Russian manufacturing processes, the bond coat metal surface is mechanically prepared in a way that is prone to removing any oxide scale formed during a prior heat treatment. It is therefore unlikely that the interfacial alumina observed originates from *ex-situ* oxidation.

2. *in-situ* bond coat oxidation during the transient pre-heat stage in vacuum.
3. *in-situ* bond coat oxidation during the transit from the pre-heat chamber to the deposition chamber in a partial pressure of oxygen, this mechanism standing for the Western type coating process.
4. *in-situ* bond coat oxidation during ceramic deposition. Bearing in mind that the ceramic is porous and that oxygen diffusivity in YSZ ceramics is significant[23] above 900°C, oxygen can be conducted to the aluminium bearing bond coat metal through the ceramic coating and fuel alumina growth.
5. *ex-situ* bond coat oxidation post ceramic deposition during heat treatments at 1050°-1100°C for times up to 4 hours. Beside oxidation from the residual oxygen present in a vacuum of 10^{-4} Torr, it is suggested that the reservoir of oxygen contained in the YSZ ceramic participates to some degree to bond coat oxidation. This suggestion follows the observation that white zirconia deposits typically darken out after a 4 hour heat treatment at 1080°C in a partial pressure of argon, implying the loss of oxygen from the ceramic.

None of the mechanisms 2 to 5 proposed above appears to have activated the oxidation of the RT31 bond coat β phase. This observation is somewhat in contradiction with a previous result reported by Leyens et al[24] who studied the effect of various pre-oxidation treatments of NiCoCrAlY bond coats. It was found that mainly the β phase was covered with oxides after a 4 hour vacuum heat treatment at 1080°C.

To account for the preferential oxidation of the bond coat gamma phase in RT31/RT33, it is proposed that the chromium rich γ phase readily forms chromia nuclei during the transient heat up stage. These nuclei would act as nucleation sites[26] and subsequent growth of alumina at a working oxygen partial pressure that is insufficient to nucleate alumina on the β phase.

It is interesting to note that the Russian process produces a continuous film of alumina between ceramic and bond coat metal whereas the Western process fails to form a continuous film, as-deposited, in spite of the oxygen bleed inside the deposition chamber.

One could argue that, prior to ceramic deposition, the flash of evaporated MCrAlY consists mainly of the γ solid solution since the time at temperature is too short to allow for extensive growth of β precipitates. The low β phase content at the time bond coat oxidation is initiated could be one argument to explain why the alumina film is continuous between KDP1 and SDP2. Moreover, the fine grain size of this MCrAlY sub-layer should promote the formation of a high density of chromia nuclei. This would further help the alumina film to cover the whole metal surface. Finally, the role of electron beam irradiation on the bond coat oxidation in the KDP1 process should not be overlooked. Electron bombardment is known to activate chemical reactions which would otherwise not take place under thermodynamic equilibrium conditions.

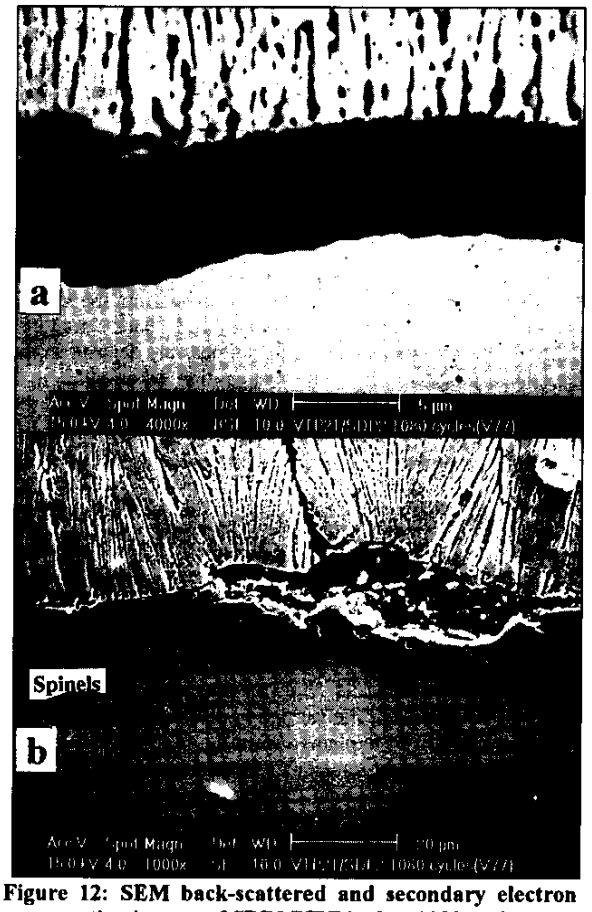

Figure 12: SEM back-scattered and secondary electron cross-section images of SDP2/KDP1 after 1080 cycles

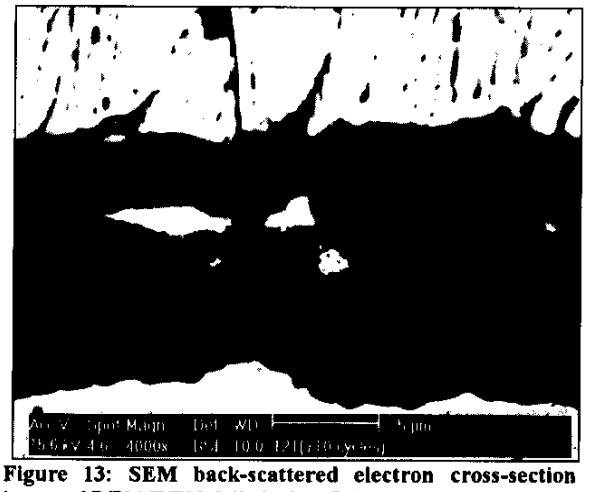

Figure 13: SEM back-scattered electron cross-section image of RT31/RT33 failed after 710 cycles.

Thermal cycling performance

EB-PVD TBC's have long been described as failing at the interface between the TGO (thermally grown oxide) and the bond coat metal[25]. It was shown in this work that a same nominal thermal barrier coating system could exhibit different spallation mechanisms ranging from a lack of adhesion at the alumina/bond coat metal to failure at the ceramic/TGO interface. Adhesive failure at the bond coat metal/TGO interface was synonymous of short cyclic lives for both the RT31/RT33 and SDP2/KDP1 systems. Whenever

the metal/oxide adhesion was good, TBC spallation life seemed to be controlled by the integrity of the ceramic/TGO interface. Failure at this interface could be the result of the formation of unprotective (Ni,Cr,Al) mixed oxides between the alumina scale and the ceramic coat as seen in the case of SDP2/KDP1. The growth of spinels at the YSZ/TGO interface implies the transport of Ni and Cr cations through the alumina scale. This could be explained by the formation of local through-cracks of the scale. No such cracks were however identified. Even in the absence of mixed oxide formation, the YSZ/alumina bond in the RT31/RT33 system seemed to deteriorate upon thermal ageing (see Figure 11). How the integrity of the YSZ/alumina interface evolves with time at temperature is an issue that may depend both on the alumina growth mechanism and ceramic sintering mechanisms.

MCrAlY coatings are known to exhibit parabolic oxidation kinetics. The scale thickness was measured on micrographs from the long life RT31/RT33 and SDP2/KDP1 systems such as those in Figures 12 and 13. Neglecting the transient oxidation on heating and cooling, estimated parabolic rate constants at 1100°C (in g^2/cm^4s) were determined based on scale thickness considerations:

System	Number of cycles	Al_2O_3 scale thickness (µm)	K_P (g^2/cm^4s)
RT31/RT33	710	7,5	$8,4 \times 10^{-13}$
SDP2/KDP1	1080	5,5	$3,9 \times 10^{-13}$

These values are consistent with published data on parabolic rate constants of bare alumina forming alloys[27].

In the absence of a fine microstructural characterization of the scales, it is difficult to account for this difference in oxidation kinetics. It is tempting though to try to correlate the higher oxidation kinetics of the RT31 bond coat to the presence of yttrium rich oxide phases within the alumina scale. The oxygen diffusivity of yttrium oxides is much higher than that of pure alumina. These yttrium rich oxides thus may act as fast oxygen diffusion paths through the scale to the bond coat/oxide interface and create as many fast growing oxidation fronts.

Bond coat oxidation kinetics is one argument to account for the superior spallation resistance of the SDP2/KDP1 system over RT31/RT33. The compressive stress within the oxide scale is maximum at room temperature. It results both from the thermal expansion mismatch between oxide and bond coat metal in addition to growth stresses. Both kinds of stresses increase with scale thickness. Moreover, under a given stress state, the probability for the scale to contain a critical flaw size also increases with scale thickness.

Whether the difference observed in ceramic morphology will also affect the spallation resistance of TBC's is a complicated issue. XRD patterns at room temperature suggest from the absence of peak shifts that EB-PVD ceramic layers contain negligible residual stresses (no more than a few hundred MPa). In another study[28], the low residual stress level in as-deposited EB-PVD ceramics was verified within the coating depth by polishing the ceramic layer.

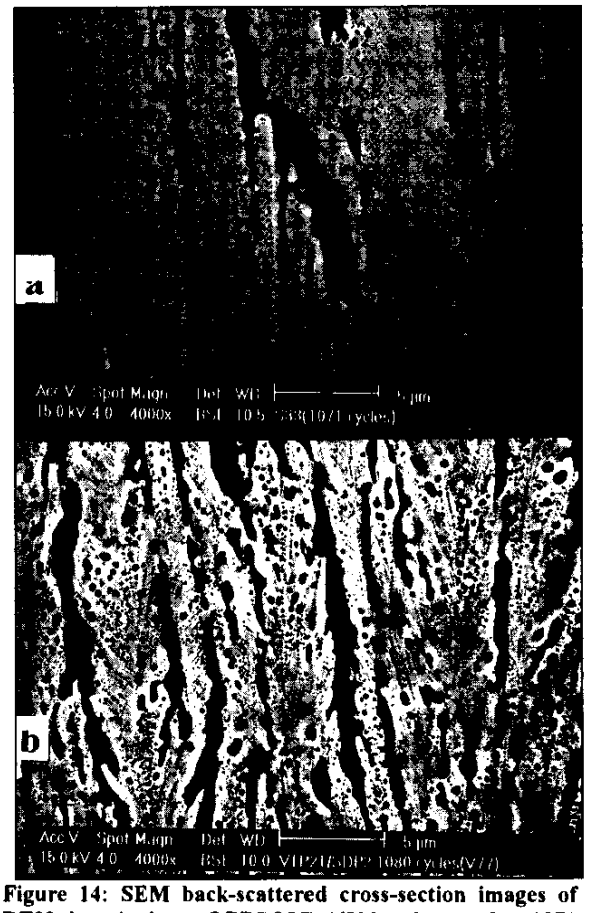

Figure 14: SEM back-scattered cross-section images of RT33 deposited on a LPPS MCrAlY bond coat after 1071 cycles (a) and KDP1 after 1080 cycles (b)

The ceramic morphology however evolves dramatically with ageing (see Figure 14 to be compared with Figure 4, both sets of pictures taken at 50 micron height from the bond coat). After more than 1000 cycles at 1100°C, sintering mechanisms have resulted in the columns branching up and microwelding together. The columnar structure is effectively partly lost. Some loss of ceramic compliance could be expected from this structural change potentially adding more stress to the TGO. This effect combined with a potential strength reduction of the ceramic/TGO interface with ageing may be responsible for the crack propagation within the region of this interface after long exposures. How the ceramic deposition process affects the integrity and stability of this interface is an open question.

CONCLUSIONS

- Western and Eastern type TBC systems exhibit different ceramic morphologies and TGO films.
- Thermal cyclic lives were found to be very scattered for both SDP2/KDP1 and RT31/RT33.
- Short lives were synonymous of lack of adhesion between TGO and bond coat metal.
- High life specimens failed in the ceramic/TGO interface region.
- The SDP2/KDP1 exhibited overall superior spallation resistance and this could be correlated to lower bond coat oxidation kinetics than in the RT31/RT33 system.

Acknowledgements: The work concerning the study of Russian TBC's was supported by the SPAÉ.The authors gratefully acknowledge the contributions of E.Célérier and M.Scher for the thermal cycling work as well as J.M.Duchemin and J.M.Thubert for the SEM work at Snecma. The X-ray diffraction studies were performed by C.Diot at Onera. Fruitful contacts and discussions with Pr Y.Tamarin at the VIAM Institute in Moscow were much appreciated. Last but not least, the authors would like to thank Rémy Mévrel at Onera for returning his useful comments on the first draft of this paper.

References

1. W.K.Halnan, D.Lee, « EB-PVD process for coating gas turbine airfoils », High temperature protective coatings 112th AIME Annual meeting, Atlanta, Georgia, March 7-8, 1983

2. S.M.Meier, D.K.Gupta, K.D.Sheffler, Ceramic TBC's for commercial gas turbine engines, JOM, March 1992

3. K.D.Sheffler, D.K.Gupta, Current status and future trends in turbine applications of TBC's, Gas Turbine Aeroengine Congress and Rxp., Amsterdam, Sep. 30 1988 ASME 88-GT-286

4. Comments from W.Goward, D.Boone, W.Halnan, TBC Workshop 1997, May 19-21, Cincinatti, Oh

5. B.A.Movchan, A.V.Demchishin, « Study of the structure and properties of thickvacuum condensates of nickel, titanium, tungsten, aluminium oxide and zirconium dioxide » Fiz.metal.metalloved.28N°4, 653-660, 1969

6. Y.Tamarin, Private communication

7. A.V.Shavkunov, Private communication

8.S.Stecura, Optimisation of NiCrAl/ZrO_2-Y_2O_3Thermal barrier system, NASA TM 86905, 1985

9.A.Feuerstein, W.Dietrich, H.Lammermann, « Advanced PVD overlay coating equipment for aircraft gas turbine engine applications », Tokyo International Gas Turbine Congress, 1987

10.H.Lammermann, A.Feuerstein, « PVD overlay coating for blades and vanes of advanced aircraft engines », 1992, Yokohama International Gas Turbine Congress

11.T.E.Strangman, »Development and performance of physical vapor deposition thermal barrier coating systems », Proceedings of the 1987 Coatings for advanced heat engine workshop III-63 to III-71, July 87

12. T.E.Strangman , US Patent 4,321,311 1982

13. N.E.Ulion, D.L.Ruckle, US Patent 4,414, 249 1983

14.B.A.Movchan, « EB-PVD Technology in the gas turbine industry:present and future », JOM November 1996

15.M.A.Smith, W.E.Frazier, B.A.Pregger, « Effect of sulfur on the cyclic oxidation behavior of a single crystalline, nickel-base superalloy », Materials science and Engineering A203 (1995) 388-398

16.D.V.Rigney, R.Viguie, D.J.Wortman, D.W.Skelly, « PVD thermal barrier coating applications and process development for aircraft engines », TBC Workshop 1995, NASA Conference publication 3312

17.Yann Jaslier, « Development of EB-PVD TBC's: the role of deposition temperature and plasma assistance », PhD thesis, Cranfield University, 1995

18.U.Schulz, K.Fritscher, H.J.Ratzer-Scheibe, W.A.Kaysser, M.Peters, « 4th Int.Symp.on high Temp. Corrosion & rotection » Mat. Les Embiez, Fr.20-24/05 1996, To be published

19. Snecma unpublished work

20. Maricocchi, Rigney, US Patent 5,350,599 Sep.1994

21.L.Lelait, S.Alpérine, C.Diot « Microstructural investigations of EB-PVD TBC's », Journal de Physique IV, Colloque C9, supplément au journal de physique III, vol 3, déc 1993

22.M.G.Scott, « Phase relationships in the zirconia-yttria system », J.Mat.Sci, 10 (1975), pp.1527-1535

23.E.C.Subbarao, « Zirconia-an overview », Science and technology of zirconia, Advances in ceramics, vol.3, A.H.Leuer, L.W.Hobbs, 1981

24.C.Leyens, K.Fritscher, R.Gehrling, M.Peters,W.A.Kaysser « Oxide scale formation on an MCrAlY coating in various H_2-H_2O atmospheres », Surface and coatings technology 82 (1996) 133-144

25.S.M.Meier, D.M.Nissley, K.D.Sheffler, T.A.Cruse, « Thermal barrier coating life prediction model development »J.Eng.Gas.Turb.&Power, 114 (1992), 258-63

26.P.Lamesle, « Revêtements d'aluminiures modifiés par le palladium:mécanismes de formation et comportement en oxydation/corrosion à haute température », Thèse de Doctorat, Université Henri Poincaré, Nancy 1, 1995

27. K.L.Luthra, C.L.Bryant, « Mechanisms of adhesion of alumina on MCrAlY alloys » Oxid.Met. 26 (5/6) 397-416 (1986)

28. Onera Rapport technique 22/3729 MY